

## PULSED LASER DEPOSITION METHOD FOR FABRICATION OF CdS/TiO<sub>2</sub> AND PbS PHOTOELECTRODES FOR SOLAR ENERGY APPLICATION

A. BJELAJAC<sup>a</sup>, V. DJOKIC<sup>b</sup>, R. PETROVIC<sup>b</sup>, G. E. STAN<sup>c</sup>, G. SOCOL<sup>d</sup>,  
G. POPESCU-PELIN<sup>d,e</sup>, I. N. MIHAILESCU<sup>d,\*</sup>, D. JANACKOVIC<sup>b</sup>

<sup>a</sup>University of Belgrade, Innovation Center of Faculty of Technology and Metallurgy, Karnegijeva 4, 11000 Belgrade, Serbia

<sup>b</sup>University of Belgrade, Faculty of Technology and Metallurgy, Karnegijeva 4, 11000 Belgrade, Serbia

<sup>c</sup>National Institute of Materials Physics, Laboratory of Multifunctional Materials and Structures, Atomistilor 105 bis, RO-077125 Magurele, Romania

<sup>d</sup>National Institute for Lasers, Plasma, and Radiation Physics, Lasers Department, "Laser-Surface-Plasma Interactions" Laboratory, Atomistilor 409, RO-077125 Magurele, Romania

<sup>e</sup>University of Bucharest, Faculty of Physics, Atomistilor 405, RO - 077125 Magurele, Romania

Titanium films sputtered on FTO glass were used for obtaining highly oriented titania nanotubes via anodization technique. Then, pulsed laser deposition of CdS was carried out for sensitizing of ~60 nm wide titania nanotubes by applying 50, 100, 150 or 200 subsequent laser pulses. Scanning electron microscopy was used to indicate which samples had the open nanotubular structure of titania preserved after the deposition of CdS. Energy dispersive spectroscopy showed that a higher number of applied laser pulses results in the increase of Cd and S quantity within samples. Pulsed laser deposition technique was also employed for the fabrication of PbS counter electrode. *I-V* characteristics of the photovoltaic cells consisting the obtained electrodes were measured and compared under one-sun illumination. The photovoltaic cell with photoanode sensitized with CdS by applying 150 laser pulses showed the highest current density and voltage among the investigated cell.

(Received November 09, 2015; Accepted December 14, 2015)

**Keywords:** Nanostructuring; Photoelectrode; Pulsed laser deposition;  
Electron microscopy studies; Sputtering.

### 1. Introduction

During recent years much attention has been paid to renewable energy sources such as solar cells. A new generation of photovoltaic cells is based upon the dye sensitized solar cell (DSSC) better known as Grätzel cell [1,2]. In order to overcome the DSSC's main disadvantage, i.e. unstable and expensive dye, the inorganic quantum dots sensitizers have been proposed as an alternative [3–10]. The photoanode layer in quantum dots sensitized solar cell (QDSSC) consists of a nanoporous TiO<sub>2</sub> film [11]. Novel nanofabricated architectures such as 1D nanotubular structures can further improve diffusion lengths in the TiO<sub>2</sub> layer while increasing the surface area for more sensitizer deposition. Furthermore, the recombination of the carriers, which commonly occurs at the boundaries of the nanoparticles, is averted in nanotubular structure [12–14]. Due to its convenient energy level with respect to TiO<sub>2</sub>, CdS is one of the most common and well-studied semiconducting sensitizers. The conduction band level of CdS is 0.5 eV above the conduction band level of TiO<sub>2</sub>. This supports a significant driving force for excited electrons to be transferred

---

\* Corresponding author: ion.mihailescu@inflpr.ro

to TiO<sub>2</sub>, increasing the probability of harvesting the excited electrons instead of recombining within CdS with photogenerated holes [15,16]. The chemical bath deposition (CBD) and successive ionic layer adsorption and reaction (SILAR) are widely used sensitization techniques due to their simplicity and low-cost [4,6,13]. As reported elsewhere [14], the CBD and SILAR methods are not able to secure the nanotubes uniform coverage with sensitizers. They often lead to the precipitation of the sensitizers inside the nanotubes or even their plugging, which consequences in the decrease of the specific surface area and adsorption capacity. The direct contact between CdS and TiO<sub>2</sub> is essential for an electron transfer with minimum energy loss. Therefore the segregation of CdS deposit could result in the decrease of the overall solar cell performance [15]. Moreover, by using these *in-situ* deposition methods it is hard to control and predict the spectral properties of the photoanodes. Thus, a new deposition technique that could be reproducible and reliable was inquired. In our previous work [17], we investigated the effectiveness of the pulsed laser deposition (PLD) method for TiO<sub>2</sub> nanotubes (NTs) array sensitization with CdS. It was shown that CdS deposited via PLD was distributed in and between nanotubes. The tuning of the optical properties of CdS/TiO<sub>2</sub> nanotubes photoanode was enabled by simple varying the number of laser pulses. The nanotubes were synthesized by potentiostatic anodization of Ti foils, but that geometry of solar cell required back-side illumination, a less efficient approach since the platinized counter electrode reflected back a significant amount of the light [18]. To enable the front-side illumination two approaches have been proposed: *i*) detachment of TiO<sub>2</sub> NTs from the Ti solid substrate and *ii*) fabrication of the TiO<sub>2</sub> NTs directly on FTO glass either using titanium isopropoxide or a two-step process: deposition of a Ti film on FTO, followed its anodization. The first method is generally being avoided since the obtained TiO<sub>2</sub> NTs film is very thin and hard to handle. We report herewith on the fabrication of transparent TiO<sub>2</sub> NTs arrays on FTO glass obtained via anodization technique. We used as starting materials a uniform, high-purity and adherent titanium films deposited by radio-frequency magnetron sputtering (RF-MS) on FTO glass.

The common QDSSC configuration includes Pt-based counter electrode, sensitized TiO<sub>2</sub> photoanode and the polysulfide electrolyte in between. However, Pt-based counter electrode exhibits poor activity in the polysulfide electrolyte. The chemical adsorption of sulfur compounds on the Pt surface may impede the electron transfer at the counter electrode/electrolyte interface resulting in less efficient solar cell structures [19]. Several alternatives to Pt and other noble metals have been suggested [20,21]. Among them, PbS was found to improve the photovoltaic parameters, compared to Pt-based electrode. Furthermore, PbS demonstrates a superior catalytic activity similar to CoS and Cu<sub>2</sub>S, but these latter materials should be avoided since they may poison the photoanode surface, thereby reducing the total cell efficiency [22]. Another remarkable advantage of PbS is its wide absorption spectrum that extends to the near infra-red region allowing the absorption of the long-wavelength light that penetrates TiO<sub>2</sub> photoanode [23]. Hence, PbS deposited on FTO glass using PLD was used in this study not only as a counter electrode, but also as a photocathode to facilitate electron injection to the electrolyte. The polysulfide electrolyte was used in this investigation since it is more compatible with the sulfide sensitizer than the iodide/triiodide redox couple, which is commonly used in DSSC [24].

This study aims to demonstrate the simplicity and feasibility of PLD method for sensitization of TiO<sub>2</sub> nanotubes with CdS as well as its use for fabrication of PbS counter electrode. The main goal of this work was studying the effect of the number of applied laser pulses on the structural properties of the photoanodes and their influence on the *I-V* characteristics of the assembled cell.

## 2. Materials and methods

### 2.1 Samples preparation

Pure titanium thin films were deposited by RF-MS onto FTO glass (PI-KEM Ltd, 200 nm FTO film, 12-14 Ω/cm<sup>2</sup>). For RF-MS, a pure titanium target (Mateck GmbH) was used. The FTO substrates were ultrasonically cleaned successively in acetone and ethanol for 10 min in an ultrasonic bath before being mechanically fixed inside the deposition chamber on an aluminum

holder at a 35 mm target-to-substrate separation distance. Prior to deposition a shadow mask was applied on the FTO glass substrate such as to obtain a coated area of 10 x 10 mm<sup>2</sup> in the sample center. The films were sputtered using a UVN-75R1 (1.78 MHz) deposition system having a magnetron cathode with a plasma ring of ~55 mm diameter. The sputtering chamber was first evacuated down to a base pressure of ~2 x 10<sup>-3</sup> Pa. Then pure argon was admitted in the reactor chamber at constant gas flow rate of 45 standard cubic centimeters per minute (sccm). Prior to deposition, the substrates were plasma etched in argon atmosphere for 10 min in order to improve films' adhesion [25]. The sputtering was carried out for 1h at a working pressure of 0.3 Pa.

The sputtered titanium films were anodized in ethylene glycol containing 0.3 wt.% ammonium fluoride and 2 wt.% water, using platinum as cathode. The electrodes were kept 20 mm apart and the voltage was set at 60 V. Real-time monitoring of the anodization current was serving for the optimization of the anodization time in order to obtain highly transparent films. After 30 min of anodization, the samples were rinsed thoroughly with water and let to dry in air for 24 h. The dried samples were annealed in air at 450 °C with a heating rate of 2 °C/min to induce crystallization of the initially amorphous nanotubes.

The UV laser source was a pulsed KrF\* excimer laser operating at 248 nm, with a pulse duration of 25 ns. The beam was focused in a spot of 10 mm<sup>2</sup> onto the surface of the CdS target at the repetition rate of 3 Hz. PLD targets were fabricated by pressing the pure CdS powders (Alfa Aesar, 99.999%) at 5 MPa in a 2 cm diameter mold at room temperature. The laser energy was set at 200 mJ, so that the incident fluence was 2 J/cm<sup>2</sup>. The residual pressure inside chamber was 2.7 x 10<sup>-3</sup> Pa and the temperature of the deposition substrate was kept at 25 °C. The substrate holder was placed parallel to the target at a 50 mm separation distance. During the laser deposition, the targets and the substrates were continuously rotated (30 rot/min) in order to avoid the piercing of the targets and to ensure the deposition uniformity. The targets were irradiated with 50, 100, 150 and 200 subsequent laser pulses and the corresponding deposited films were labeled accordingly as NT50, NT100, NT150 and NT200, respectively.

The PbS targets were fabricated by sintering the pure PbS powder (Sigma Aldrich, 99.9%) at 5 MPa in a 2 cm diameter mold at room temperature. The same deposition conditions were used as for CdS, except for the number of laser pulses which was set in this case at 1500.

## 2.2 Characterization techniques

The samples structure were examined by X-ray diffraction (XRD) using a Bruker D8 Advance diffractometer with CuK<sub>α</sub> ( $\lambda = 1.5418 \text{ \AA}$ ) radiation. In order to enhance the signal coming from the samples' surface, the patterns were recorded in grazing incidence (GIXRD) geometry. The incidence angle was set to 2°, and the scattered intensity was scanned within the 2 $\theta$  angular range 20–65°, with a step size of 0.04°, and an acquisition time of 10–110 s.

Scanning electron microscopy (SEM) investigations were performed with a Vega Tescan instrument under secondary electrons mode. Additionally, field emission scanning electron microscopy (FESEM) analyses were carried out by employing a Mira X3 Tescan instrument.

Compositional analyses were performed by energy dispersive spectroscopy (EDS) using a Jeol 5800 apparatus.

CdS sensitized TiO<sub>2</sub> photoanodes when sealed with a PbS/FTO counter electrodes using a 0.2 mm spacer. The liquid polysulphide (0.5 M Na<sub>2</sub>S, 2 M S, 0.2 M KCl in methanol to water ratio of 7:3) electrolyte was injected between the electrodes. The photocurrent-voltage (*I-V*) characteristics of solar cells were recorded under 100 mW/cm<sup>2</sup> illumination by a Thermal Oriel solar simulator (L.O.T.-ORIEL GmbH & Co. KG). The electrical properties were measured with a Keithley 6487 picoammeter/voltage source.

## 3. Results and discussion

Fig. 1 displays a typical top-view SEM micrograph of an as-sputtered titanium film. The SEM analyses revealed well-adhered films with a homogeneous nanostructured surface, consisting of merged nanograins, having the average diameter of ~200 nm. No signs of either microcracks or delaminations were noticed. Fig. 1-inset presents the cross-view SEM image of the titanium film.

One can observe that the  $\sim 1.6 \mu\text{m}$  thick film has a columnar structure, typical for RF-MS films grown at room temperature.

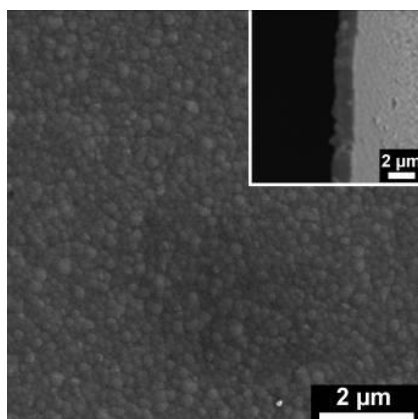


Fig. 1: Typical SEM surface and cross-sectional morphology (inset) of as-sputtered titanium films

Fig. 2 shows FESEM micrographs of the surface microstructure of Ti film coated on the FTO glass substrate after the anodization, revealing the  $3.5 \mu\text{m}$  long  $\text{TiO}_2$  nanotubes with a  $\sim 60 \text{ nm}$  inner diameter. Compared to the thickness of the Ti film ( $\sim 1.6 \mu\text{m}$ ) the length of the nanotubes is increased due to the high porosity of  $\text{TiO}_2$  film. The transparency of the obtained  $\text{TiO}_2$  films is indicative for the Ti amount consumed in formation of  $\text{TiO}_2$  layer.

In our previous study [17], it was shown that 250 and 500 laser pulses were sufficient to sensitize  $\sim 100 \text{ nm}$  wide nanotubes. Therefore, herein for narrower pores structure the number of the laser pulses was set to 200 and lower.

Fig. 3 gives the overview of the FESEM images of the  $\text{TiO}_2$  nanotubes after the CdS deposition, corresponding to different number of pulses. For the samples NT50, NT100 and NT150 one can notice that the nanotubular structure remains open without clogging, which ensures the electrolyte penetration for further assembly of the cells. However, in the case of the NT200 samples the excess of CdS is noticed, which now obturates the  $\text{TiO}_2$  nanotubes, whose typical morphology is hard to discriminate. Such situation should be avoided since it can cause the increase of the recombination of the electron-hole pairs [15]. By decreasing the distance that charge carriers should cross inside the sensitization layer to reach the electrolyte or the underlying  $\text{TiO}_2$ , the recombination of the electron-hole pairs can reach a minimum. Therefore, the sample NT200 was excluded from the further investigations.

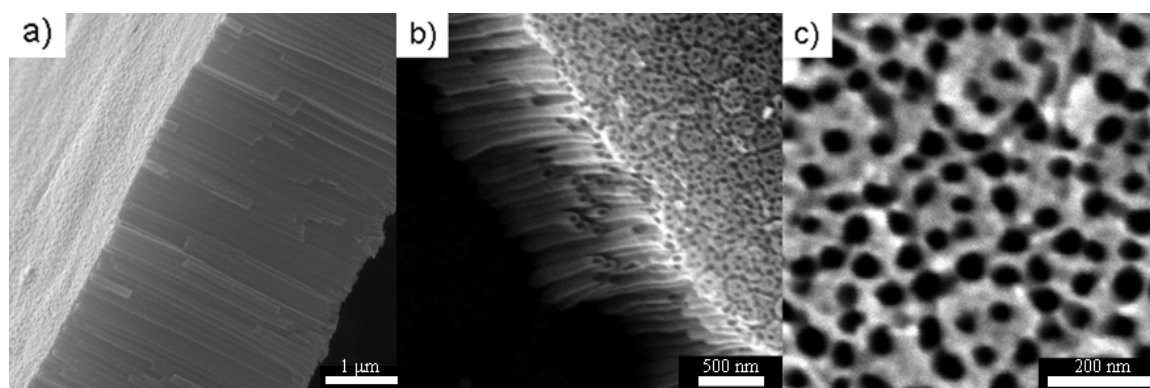


Fig. 2: SEM micrographs of as-prepared  $\text{TiO}_2$  nanotubes: (a) cross-view image showing the nanotubes length of  $3.5 \mu\text{m}$ ; (b) tilt-view image presenting more clearly the  $\text{TiO}_2$  nanotubes' structure; and (c) top-view image highlighting the inner diameter ( $\sim 60 \text{ nm}$ ) of the nanotubes

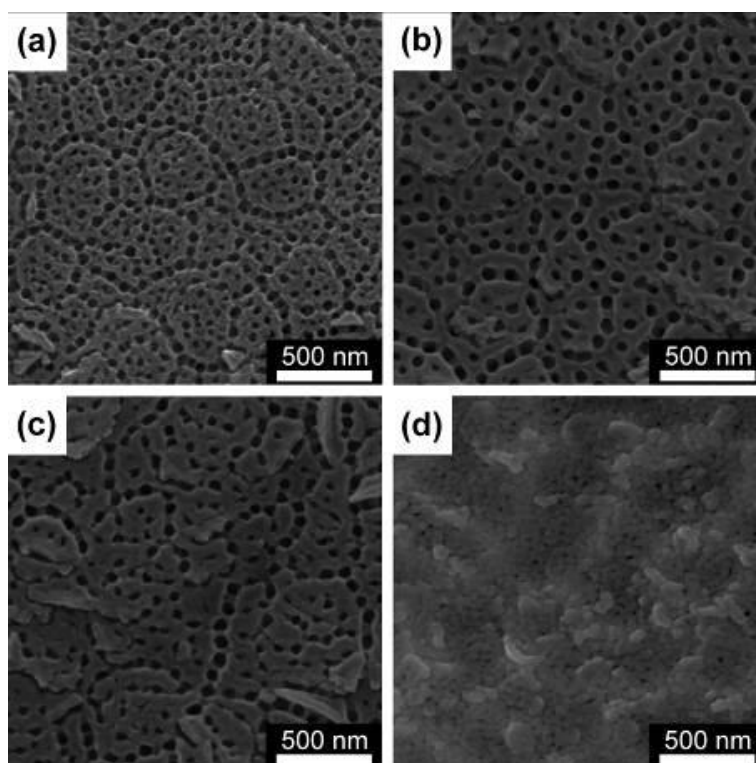


Fig. 3: Typical FESEM images of the: (a) NT50, (b) NT100, (c) NT150 and (d) NT200 samples

By comparing Fig. 3 to Fig. 2, a certain narrowing of the nanotubes diameter can be observed as a consequence of CdS coverage by PLD. From the FESEM micrographs (Fig. 3) the inner diameter was estimated as: a)  $\sim 55$  nm (NT50), (b)  $\sim 50$  nm (NT100) and (c)  $\sim 45$  nm (NT150). As it was shown in Ref. [17], the CdS sensitization of  $\text{TiO}_2$  nanotubes via PLD technique is properly distributed over the entire nanotubes walls surface. We therefore focused, in the frame of this study, on the top view FESEM investigations only.

The results of EDS study of NT50, NT100 and NT150 samples, are collected in Table 1. It is obvious that the amount of CdS deposit increases with the number of laser pulses applied for deposition. One notes that Si and Sn signals originate from FTO substrates.

Table 1: Chemical composition (at. %) of NT50, NT100 and NT150 samples, inferred by EDS analysis

Element	Sample		
	NT50	NT100	NT150
O	$74.25 \pm 0.29$	$73.16 \pm 0.24$	$72.59 \pm 0.23$
Si	$0.08 \pm 0.02$	$0.11 \pm 0.02$	$0.08 \pm 0.02$
S	$0.10 \pm 0.04$	$0.15 \pm 0.02$	$0.31 \pm 0.02$
Ti	$25.33 \pm 0.27$	$26.27 \pm 0.24$	$26.60 \pm 0.23$
Cd	$0.10 \pm 0.02$	$0.16 \pm 0.03$	$0.27 \pm 0.03$
Sn	$0.12 \pm 0.01$	$0.14 \pm 0.02$	$0.15 \pm 0.03$

The GIXRD analysis (Fig. 4) of the obtained CdS/NT150/FTO photoanodes showed clearly that  $\text{TiO}_2$  nanotubes had a majoritary anatase structure (ICDD: 00-021-1272). Traces of a titanium sub-oxide phase ( $\text{Ti}_6\text{O}$  – ICDD: 01-072-1471) have been also evidenced. The diffraction peaks of CdS deposits were difficult to emphasize due to the low amount of CdS and the partial overlapping of its diffraction lines on the prominent diffracted signals originating from the anatase

nanotubes arrays and the bottom FTO conductive substrate (ICDD: 01-077-0452). In order to tackle this problem, and assess the nature of the PLD deposits, GIXRD investigations have been performed on CdS structures deposited under the same working conditions onto bare silica glass substrates. This way by performing overnight measurements it was allowed the detection of CdS phase, but only for the sample prepared by applying a higher number (150) of laser pulses. The GIXRD patterns of NT100 and NT150 are presented comparatively in Fig. 4-inset.

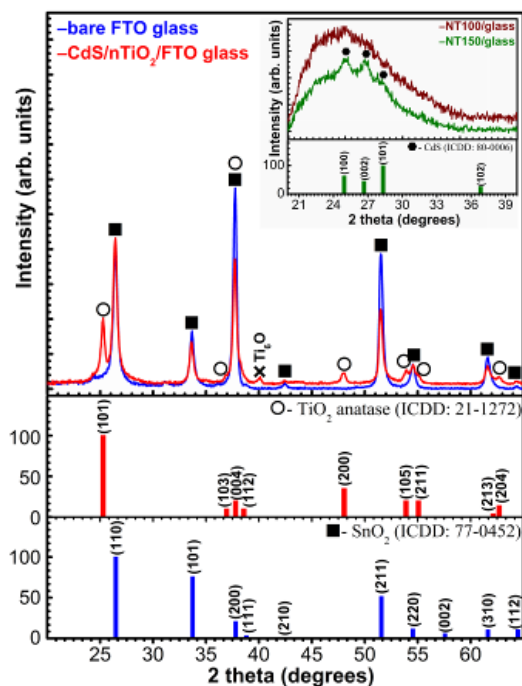


Fig. 4: Typical XRD pattern of CdS/NT150/FTO photoanode. Inset: XRD diagrams of CdS structures deposited onto bare glass substrate by applying 100 and 150 laser pulses. The ICDD reference files of TiO<sub>2</sub>-anatase, SnO<sub>2</sub> and CdS are also inserted for comparison

One can observe the broadened diffraction peaks (characteristic of a nanosized material) corresponding to a hexagonal CdS phase (ICDD: 01-080-0006), superimposed on the amorphous halo assigned to the silicate glass structure. A *c*-axis preferential orientation of CdS deposit, in the case of NT150, is suggested by the increase of the 002 line intensity with respect to the reference diffraction file (ICDD: 01-080-0006), and the strong diminution of the highest intensity line (101) of the hexagonal CdS phase. No diffraction maxima could be emphasized in the case of NT100 sample, measured in identical conditions (Fig. 4-inset), due to the reduced amount of pulsed laser deposited CdS material, situated under the sensitivity limit of the XRD machine employed in this study.

After injecting the electrolyte between the assembled electrodes, the cells *I*-*V* performance parameters were measured both in dark and illumination with simulated sunlight at 1.5 AM (100 mW/cm<sup>2</sup>). All solar cells evidenced the photovoltaic effect as visible from the graphs presented in Fig. 5.

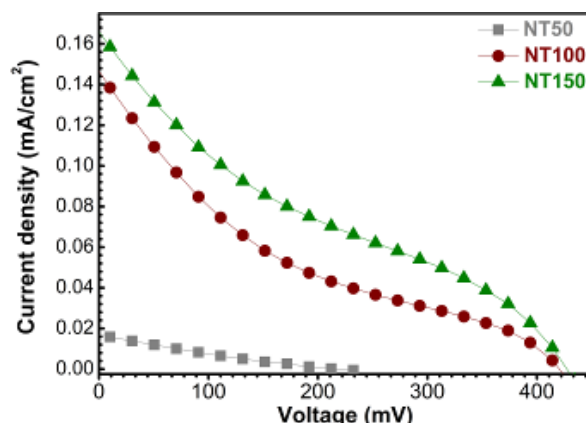


Fig. 5: *I-V characteristics of the photovoltaic cells with NT50, NT100 and NT150 photoanodes*

By comparing the graphs enclosed in Fig. 5, it is obvious that when the amount of the CdS deposit increases the current density and voltage increase. However the shape of the curves indicates the low value of the fill factors ( $\sim 0.20$ ) which can be attributed to the poor hole-recovery rate of polysulphide, leading to a high rate of surface recombination at the QD/electrolyte interface [26]. Our study emphasized the 150 laser pulses as the optimal value for the CdS deposition within the  $\sim 60$  nm wide TiO<sub>2</sub> nanotubes arrays. At lower numbers of pulses the photovoltaic cell parameters decline, whilst at the higher number of pulses the nanotubes are clogged.

The pulsed laser deposition method was also used to obtain a PbS counter electrode. Its wide absorption range (300-700) nm is shown in Fig. 6 where the additional transmittance spectrum of CdS thin film is given for comparison. This result points to the advantage of use PbS as a counter electrode since it provides additional amount of excited electrons that TiO<sub>2</sub> photoanode was not able to absorb [23]. PbS here serves therefore as a photocathode in this configuration of the solar cell.

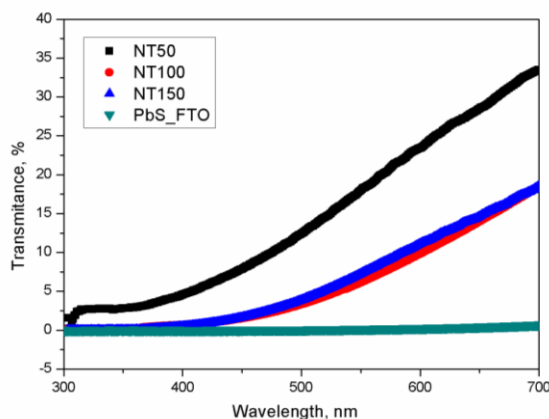


Fig. 6: *UV-VIS transmission spectra of CdS versus PbS thin films within the (300-700) nm spectral range*

#### 4. Conclusions

We demonstrated that the pulsed laser deposition of CdS for sensitization of titania photoanode can be tailored by changing the number of laser pulses, suggesting that this less explored technique is a promising alternative for the CdS deposition. Under one-sun illumination, the *I-V* characteristics of the assembled solar cells were measured and the best photovoltaic performance has been obtained in the case of cells with TiO<sub>2</sub> nanotubes sensitized with CdS by applying 150 laser pulses.

A complete absorption of light within (300-700) nm spectrum was observed in case of PbS films playing an advantageous role as a photocathode.

### Acknowledgements

The Serbian authors acknowledge with thanks the financial support of the Ministry of Education, Science and Technological Development, Republic of Serbia through the Projects III 45019. Romanian authors acknowledge with thanks the financial support of UEFISCDI under the contract ID 304/2011. GES is grateful for the support of PN09-45010 Core Programme.

### References

- [1] S. Ruhle, A. Y. Anderson, H. N. Barad, B. Kupfer, Y. Bouhadana, E. Rosh-Hodesh, A. Zaban, *J. Phys. Chem. Lett.* **3**, 3755 (2012).
- [2] K. Govardhan Reddy, T. G. Deepak, G. S. Anjusree, S. Thomas, S. Vadukumpully, K. R. V. Subramanian, Shantikumar V. Nair, A. Sreekumaran Nair, *Phys. Chem. Chem. Phys.* **16**, 6838 (2014).
- [3] I. Hod, V. Gonzalez-Pedro, Z. Tachan, F. Fabregat-Santiago, I. Mora-Sero, J. Bisquert, A. Zaban, *J. Phys. Chem. Lett.* **2**, 3032 (2011).
- [4] S. Ruhle, M. Shalom, A. Zaban, Quantum-dot-sensitized solar cells, *Chem. Phys. Chem.* **11**, 2290 (2010).
- [5] G. Hodes, *J. Phys. Chem. C* **112**, 17778 (2008).
- [6] I. Hod, A. Zaban, *Langmuir* **30**, 7264 (2014).
- [7] H. K. Jun, M. A. Careem, A. K. Arof, *Renew. Sust. Energ. Rev.* **22**, 148 (2013).
- [8] Prashant V. Kamat, *J. Phys. Chem. C* **112**, 18737 (2008).
- [9] Y. Jin-nouchi, S. Naya, H. Tada, *J. Phys. Chem. C* **114**, 16837 (2010).
- [10] H. Joong Lee, J. H. Yum, H. C. Leventis, S. M. Zakeeruddin, S. A. Haque, P. Chen, S. I. Seok, M. Gratzel, Md. K. Nazeeruddin, *J. Phys. Chem. C* **112**, 11600 (2008).
- [11] D. A. H. Hanaor, C. C. Sorrell, Review of the anatase to rutile phase transformation, *J. Mater. Sci.* **46**, 855 (2011).
- [12] S. Chen, M. Paulose, C. Ruan, G. K. Mor, O. K. Varghese, D. Kouzoudis, C. A. Grimes, *J. Photochem. Photobiol. A-Chem.* **177**, 177 (2006).
- [13] W. Sun, Y. Yu, H. Pan, X. Gao, Q. Chen, L. Peng, *J. Am. Chem. Soc.* **130**, 1124 (2008).
- [14] Y. Lai, Z. Lin, D. Zheng, L. Chi, R. Du, C. Lin, *Electrochim. Acta* **79**, 175 (2012).
- [15] M. Qorbani, N. Naseri, O. Moradlou, R. Azimirad, A.Z. Moshfegh, *Applied Catalysis B: Environmental* **162**, 210 (2015).
- [16] S. Emin, S. P. Singh, L. Han, N. Satoh, A. Islam, *Solar Energy* **85**, 1264 (2011).
- [17] A. Bjelajac, V. Djokic, R. Petrovic, G. Socol, I. N. Mihailescu, I. Florea, O. Ersen, Dj. Janackovic, *Appl. Surf. Sci.* **309**, 225 (2014).
- [18] K. Das, S. K. De, *J. Phys. Chem. C* **113**, 3494 (2009).
- [19] Y. Lee, Y. Lo, *Adv. Funct. Mater.* **19**, 604 (2009).
- [20] M. Seol, E. Ramasamy, J. Lee, K. Yong, *J. Phys. Chem. C* **115**, 22018 (2011).
- [21] Z. Yang, C. Y. Chen, C. W. Liu, C. L. Li, H. T. Chang, *Adv. Energy Mater.* **1**, 259 (2011).
- [22] Z. Tachan, M. Shalom, I. Hod, S. Ruhle, S. Tirosh, A. Zaban, *J. Phys. Chem. C* **115**, 6162 (2011).
- [23] C. Lin, C. Teng, T. Li, Y. Lee, H. Teng, *J. Mater. Chem. A* **1**, 1155 (2013).
- [24] P. Lekha, A. Balakrishnan, K. R. V. Subramanian, S. V. Nair, *Mater. Chem. Phys.* **141**, 216 (2013).
- [25] A.C. Galca, G.E. Stan, L.M. Trinca, C.C. Negrila, L.C. Nistor, *Thin Solid Films* **524**, 328 (2012).
- [26] H. Lin, C. P. Huang, W. Li, C. Ni, S. Ismat Shah, Y. H. Tseng, *Appl. Catal. B-Environ.* **68**, 1 (2006).